Received: 2 August 2021 | Revised: 17 February 2022 | Accepted: 19 March 2022

DOI: 10.1002/hyp.14563

THE ROLE OF BIG DATA AND MACHINE LEARNING IN HYDROLOGICAL PROCESSES

WILEY

Understanding event runoff coefficient variability across Australia using the *hydroEvents R* package

Conrad Wasko | **Danlu Guo**

Department of Infrastructure Engineering, The University of Melbourne, Parkville, Australia

Correspondence
Conrad Wasko, Department of Infrastructure Engineering, The University of Melbourne, Parkville, Australia.
Email: conrad.wasko@unimelb.edu.au

Funding information
Australian Research Council, Grant/Award Number: DE210100479

Abstract

Identification and pairing of hydrologic events form the basis of various analyses, from identifying events for the calibration of hydrologic models, to calculation of event runoff coefficients for catchment characterization. Despite this, there is no unified approach for identifying hydrologic events. Here, using the *R* package, *hydroEvents* (https://CRAN.R-project.org/package=hydroEvents), we compare multiple methods of extracting and pairing hydrologic events focussing on the relationship between rainfall and runoff. We find the four common analytical approaches used to identify runoff events—based on either event threshold, local maxima/minima, or proportion of baseflow contribution, give similar results. However, when rainfall events are paired to runoff, the type of algorithm and the direction of pairing (either from rainfall to runoff, or runoff to rainfall) make a considerable difference to the final event pairs identified and resulting analyses. Here, we demonstrate the value of automated event extraction and pairing algorithms for large-sample hydrology analysis by calculating event runoff coefficients across Australia. Our results show that climatology is a key driver of catchment rainfall-runoff response with much of Australia dominated by excess rainfall runoff generation. However, our results also show that the variability due to pairing method can introduce a variability equal to that of the climatology due to biasing the runoff mechanism within the sample. With this analysis we demonstrate the importance of systematic and consistent approaches to hydrologic characterization when identifying and pairing hydrological events.

KEYWORDS
baseflow, event delineation, event identification, precipitation, rainfall-runoff, runoff coefficient, streamflow

1 | INTRODUCTION

Hydrologic events, such 'pulses' or 'peak periods' of rainfall or streamflow, have important environmental and ecological functions (Frazier et al., 2003; Tonkin et al., 2019). On the one hand, extreme precipitation events can cause flooding and risk to life (Razavi et al., 2020; Wasko et al., 2021a), but on the other hand, a lack of precipitation events can result in drought, water scarcity, and threaten agricultural production (Vogel et al., 2019). The calculation of hydrologic event characteristics such as event runoff coefficients can describe runoff generation processes and classify catchment behaviour (Merz et al., 2006; Tarasova et al., 2018; McMahon and

Nathan, 2021). Calculating the water quality during periods of streamflow events and baseflow helps understand the source and transport of contaminants (Minaudo et al., 2019; Guo et al., 2022). Streamflow events are used to calibrate hydrologic models (Tramblay et al., 2010; O'Shea et al., 2021) while streamflow recessions are used to estimate hydraulic conductivity, storage capacity, aquifer thickness (Stoelzle et al., 2013), and reconstruct precipitation (Kirchner, 2009). Hence, the identification and characterization of hydrologic events is crucial to our understanding of catchment hydrology and hydrologic applications such as flood forecasting, flood protection, and water resource and quality management.

A hydrologic event is generally identified as a sequence of continuous observations above a certain threshold with a given separation time between subsequent events. For example, rainfall events are routinely identified using a peaks over threshold (POT) approach, with non-zero rainfall separated by a rainless minimum inter-event time (Dunkerley, 2008). However, when identifying streamflow events, there remains streamflow in the system not directly related to the precipitation event, termed baseflow, which needs to be removed for event separation. As tracer or water balance modelling experiments are required to accurately identify the source of streamflow (Partington et al., 2012; Ladson et al., 2013; Li et al., 2013; Zhang et al., 2020; Yao et al., 2021), baseflow separation practice remains largely empirical (Linsley et al., 1958). Graphical methods of baseflow separation either: i) extend the recession prior to a storm to a point at the end of the surface runoff; or ii) project from after the storm back to a point of inflexion of the falling limb and match the start of the runoff with a smooth curve (Linsley et al., 1958; Raudkivi, 1979). Graphical methods however are often manual and hence not practical for large sample studies. Due to the ease of use in computational studies, digital filters (Lyne and Hollick, 1979) are now the most common method for baseflow separation. But, baseflow separation is not sufficient to identify streamflow events, particularly in small catchments (Hewlett and Hibbert, 1967). Therefore, additional approaches are often used to identify streamflow events including turning points and fractional baseflow ratios (Merz et al., 2006; Sikorska et al., 2015; Kaur et al., 2017; Tang and Carey, 2017; Tarasova et al., 2018).

In addition to identifying hydrologic events from individual time series, there is a need to pair events from multiple time series. Climatic catastrophes are often the result of extremes in multiple variables such as rainfall and a high tide coinciding in space and time (Leonard et al., 2014) and their coincidence needs to be considered in engineering design (Wasko et al., 2021b). Groundwater level response to rainfall and streamflow is an indicator of the level of interconnectedness of the surface and groundwater system (Zimmer and McGlynn, 2017). Rainfall-runoff partitioning (Saft et al., 2016; Peterson et al., 2021) is critical to classifying catchment response and when performed on an event basis relies on pairing rainfall to the corresponding runoff (Blume et al., 2007). Understanding the drivers of flooding and attributing trends in flood response also relies on accurate pairing of rainfall-runoff events (Merz et al., 2012).

The choice of event identification and pairing approach can lead to differing results in the subsequent hydrologic analyses and applications (Blume et al., 2007). For example, if independent events are not properly identified, additional serial correlation will be introduced and trends artificially detected when none are present (von Storch, 1999). As there is no unified approach to identifying hydrologic events, the implementation of multiple automated approaches for event identification and pairing, especially in the application of large-sample analyses, is preferable. Several software tools exist for identifying and pairing hydrologic events (Table 1). Most packages focus on baseflow separation, with few packages identifying or pairing events. While *HydRun* (Tang and Carey, 2017) does pair events, this is performed on the basis of runoff response, but, as Wasko and Nathan (2019) noted, pairing based on precipitation is necessary for ensuring antecedent conditions are independent of the runoff response. The *R* package *hydroEvents* (Wasko and Guo, 2021) is the only package which implements multiple event identification and pairing strategies, including pairing in different search directions (e.g. from rainfall to runoff, or from runoff to rainfall).

Existing large-scale studies of event runoff responses are largely focused on catchments in temperate climates in Europe and North America (Cerdan et al., 2004; Merz et al., 2006; Tarasova et al., 2018; Stein et al., 2020). This means the climate conditions explored so far for event runoff responses are rather narrow, potentially limiting transferability to other climate zones and parts of the world due to the critical role of climate in controlling catchment hydrological regimes (Beck et al., 2013). Therefore, this study aims to explore the event rainfall-runoff relationship across a wide range of climatic conditions, considering multiple methods of extracting and pairing hydrologic events. Here, we use the *R* package *hydroEvents* (Wasko and Guo, 2021), which samples and pairs hydrologic events in a flexible and parsimonious manner, to calculate event runoff coefficients for the first time on a continental scale across Australia. We first test the event identification and pairing algorithms, before calculating runoff coefficients across Australia and comparing the results to annual rainfall-runoff relationships. Finally, the impact of climate variability, catchment area, and pairing strategy on the calculated runoff coefficients is examined.

2 | DATA

We apply *hydroEvents* to calculate event runoff coefficients for the 467 Hydrologic Reference Stations (HRS) across Australia. The HRS are the highest-quality, unimpacted daily streamflow stations for the continent of Australia (Zhang et al., 2016) and are presented in Figure 1 underlain by the Köppen Climate classification (Beck et al., 2018). Missing data is infilled using hydrologic modelling (Zhang et al., 2016). The record lengths vary from 30 to 69 years with a median record length of 48 years. Catchment average rainfall is calculated from the Australian Water Availability Project (AWAP), a $0.05^\circ \times 0.05^\circ$ daily gridded rainfall derived from surface gauging (Jones et al., 2009) using the *R* package *AWAPer* (Peterson et al., 2020). The rainfall and streamflow records are restricted to the nearest complete water year, where the start of water year is defined as the first day of the month which has the lowest monthly average flow (Wasko et al., 2020a).

TABLE 1 Summary table of selected packages performing hydrologic event separation

Package name	Code	Summary of event analysis	Reference
Baseflow	R	Computes hydrograph separation an automated process (Pelletier and Andréassian, 2020). Does not explicitly identify events.	(Pelletier et al., 2021)
BaseJumper	-	Computes baseflow using a Lyne-Hollick (Lyne and Hollick, 1979) baseflow filter. Does not explicitly identify events.	(Sinclair Knight Merz, 2007)
BFLOW	-	Computes baseflow using a Lyne-Hollick (Lyne and Hollick, 1979) baseflow filter. Does not explicitly identify events.	(Arnold and Allen, 1999)
AQUAPAK	-	Applies a Lyne-Hollick (Lyne and Hollick, 1979) baseflow filter. Calculates and reports on spells above and below a threshold.	(Nathan et al., 2007)
EcoHydRology	R	Applies a Lyne-Hollick (Lyne and Hollick, 1979) baseflow filter. Does not explicitly identify events.	(Fuka et al., 2018)
FlowScreen	R	Implements three different recursive digital filters for separating baseflow (Boughton, 1993; Eckhardt, 2005, 2012). Identifies flow peaks over a given threshold within a minimum separation between peaks and annual maxima. Does not identify the start and end of events.	(Dierauer and Whitfield, 2019)
HydroEvents	R	Removes baseflow using a Lyne-Hollick (Lyne and Hollick, 1979) baseflow filter. Identifies hydrologic events using four different algorithms including peaks over threshold, the difference between neighbouring peaks, the difference between neighbouring values, and baseflow fraction. Events (e.g. rainfall to runoff) are paired using one of five event pairing algorithms.	(Wasko and Guo, 2021)
Hydromad	R	Identifies events by identifying when data exceeds a certain threshold. The event lasts until a lower threshold is met.	(Andrews et al., 2011)
Hydrostats	R	Applies a Lyne-Hollick (Lyne and Hollick, 1979) baseflow filter. Calculates a range of high and low spell statistics over a specified quantile but does not return the events themselves.	(Bond, 2019)
HydRun	Matlab	Removes baseflow using a Lyne-Hollick (Lyne and Hollick, 1979) baseflow filter. Identifies high flow events based on absolute difference between their neighbouring valleys and then matches these events to rainfall events.	(Tang and Carey, 2017)
IETD	R	Computes statistics of independent rainfall events. Calculates independent inter-event time estimates based on three different methods (Joo et al., 2014).	(Duque, 2020)
Lfstat	R	Can identify low flow periods below a threshold along with flow statistics. Baseflow separation is present (Tallaksen and van Lanen, 2004) but individual events are not identified.	(Koffler et al., 2016)
SAAS	Matlab	Identifies high flow events based on absolute or relative differences between the peaks and their neighbouring valley. Criteria for rising and falling limbs and magnitude can be included.	(Metcalfe and Schmidt, 2016)
WAFO	Matlab	Toolbox statistical analysis and simulation of random waves and random load that includes a POT algorithm.	(Brodtkorb et al., 2000)

With reference to the Köppen climate classification (Figure 1), Australia's climate is tropical (A) in the north, temperate (C) on the east and southern coasts, and arid (B) inland. There is a small region in the northeast which is classified as temperate with a dry winter (Cw) and closely resembles the tropical region, though experiencing greater mean rainfalls due to advection of moisture

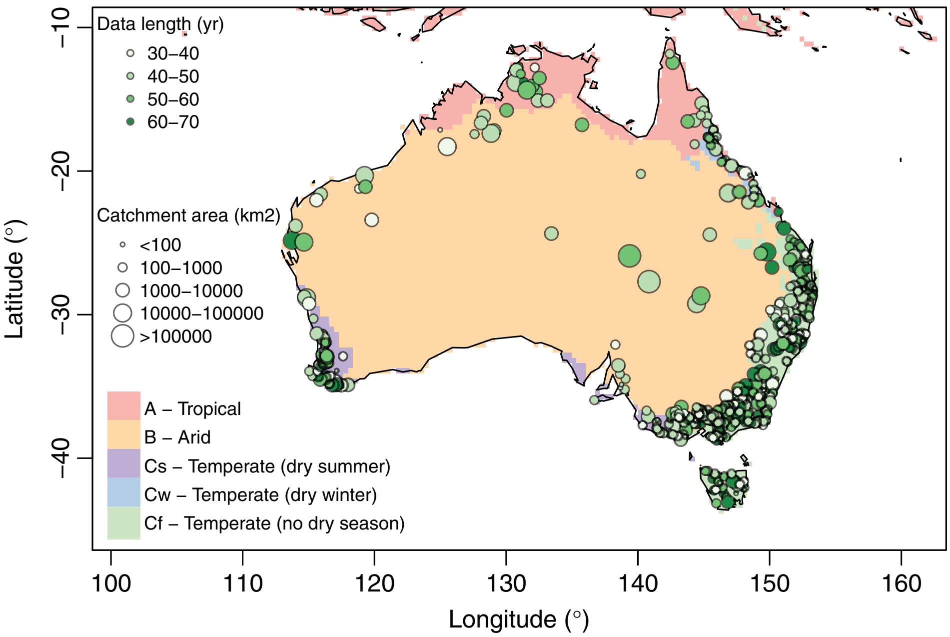

FIGURE 1 Hydrologic Reference Station location, record length, and catchment area. The gauging stations are underlain by the Köppen climate classification (Beck et al., 2018)

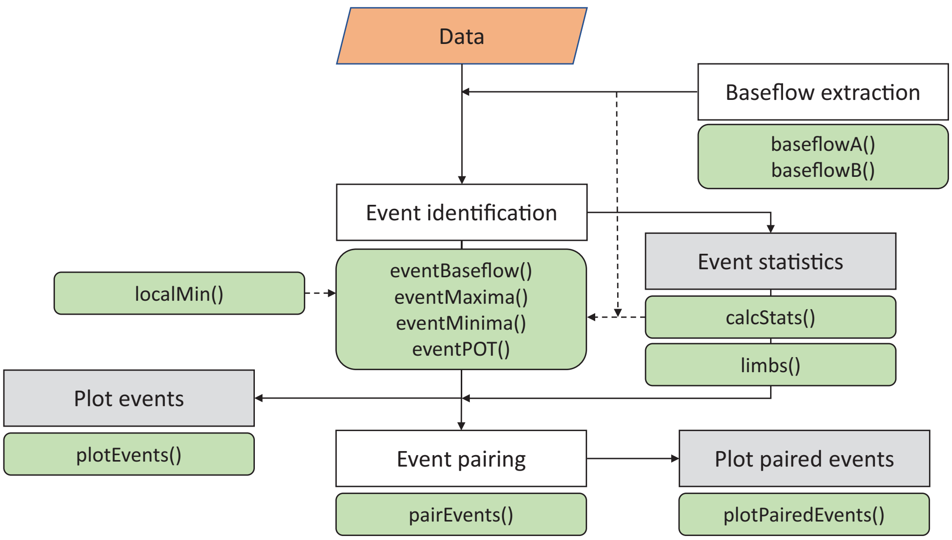

FIGURE 2 Schematic of the features in *hydroEvents*. The only input is the data (orange) with the primary (white) and secondary (grey) workflow steps following the arrows. The functions (green) attached to each step are shown. Dashed arrows represent dependencies within the package that are not directly called by the user

via southeast trade winds. The south-east temperate region has no dry season (Cf) while the south-east has a dry summer (Cs). Most HRS stations are located along the coast in the temperate and tropical regions.

3 | THE HYDROEVENTS PACKAGE

The *hydroEvents* package (Wasko and Guo, 2021) available via CRAN at: https://CRAN.R-project.org/package=hydroEvents is an open-source package for extracting and pairing hydrologic events written in the *R* programming language. The sole input is a vector of continuous data with the package built around two main features: event identification and event pairing (Figure 2). Either before or after baseflow separation (Section 3.1) events are identified using one of four methods (Section 3.2), and then, if event identification has been performed on multiple data sets, the events can be paired using one of five pairing specifications (Section 3.3).

Here we calculate event runoff coefficients using the *calcStats()* function which can pass any user defined function to calculate event statistics. For ease of use, functions for plotting both the single and paired events are also provided via *plotEvents()* and *plotPairedEvents()* and are used here to generate the resulting plots. Although not used in calculating runoff coefficients, *limbs()* can be used to perform rising and falling limb identification to enable further fine-scale analyses that focus on individual parts of the hydrographs, for example, to assess the relationship of water quality and runoff at the rising and falling limbs (Bende-Michl et al., 2013).

3.1 | Baseflow separation

The are many methods for separating baseflow from streamflow with new methods regularly being introduced (Chen and Teegavarapu, 2019; Pelletier and Andréassian, 2020). *HydroEvents* uses the one-parameter recursive digital filter (Lyne and Hollick, 1979) as it is the most prevalent baseflow filter in the literature and arguably the most parsimonious (Nathan and McMahon, 1990; Eckhardt, 2008). The digital filter can be described by (Lyne and Hollick, 1979):

$$f_k = \alpha f_{k-1} + \frac{(1+\alpha)}{2}(y_k - y_{k-1}) \quad (1)$$

where f_k is the filtered quick response at the kth sampling point, y_k is the original streamflow and α is the filter parameter. The baseflow is hence the difference between the original streamflow y_k and the quickflow f_k.

HydroEvents implements the one-parameter recursive digital filter to separate the streamflow into the baseflow and quickflow in the functions *baseflowA()* and *baseflowB()*. The implementations of *baseflowA()* (Fuka et al., 2018) and *baseflowB()* (Ladson et al., 2013) are identical to the cited authors. The majority of literature recommend for daily streamflow a baseflow filter parameter (α) of 0.925 with three passes (Nathan and McMahon, 1990). The reason for implementing two baseflow filters is that the literature describing each of these baseflow filters suggests the implementations are the same. However, when one inspects the code, it is noted that Fuka et al. (2018) adopts an algorithm with baseflow as the subject and updates the quickflow at each time step whereas Ladson et al. (2013) implements an algorithm using quickflow as the subject and updates the baseflow at the end of each pass.

3.2 | Event identification

Events are extracted using either event threshold, local maxima/minima or the proportion of baseflow. A schematic of each of the methods is presented in Figure 3 with each of the identification methods outlined below. Identified events are plotted using *plotEvents()*.

3.2.1 | Peaks over threshold

In the method of sampling commonly referred to as a 'peaks over threshold' approach, and implemented in the function *eventPOT()* within *hydroEvents*, only data above a certain value (*threshold*) are considered events, with events spaced by a minimum number of time steps (*min.diff*). A common application is to identify rainfall events as non-zero rainfall with a specified minimum interevent time between events. Criteria for selecting rainfall events varies depending on the event of interest and the minimum interevent time can range from several minutes to days (Dunkerley, 2008; Xuereb and Green, 2012; Wasko et al., 2022), but generally a threshold of the instrument precision is used for sub-daily rainfall with an inter-event time of ~3 h (Molnar et al., 2015; Visser et al., 2020). For daily rainfall, studies have generally used a threshold of 1 mm and 1 day of zero rainfall (Wasko and Nathan, 2019). The peaks over a threshold approach is also frequently applied for extracting wave heights, flood levels and spell characteristics of rainfall and temperature.

3.2.2 | Local maxima

Implemented in the function *eventMaxima()*, peaks are first identified and then the relative (or absolute) difference (*delta.y*) to the

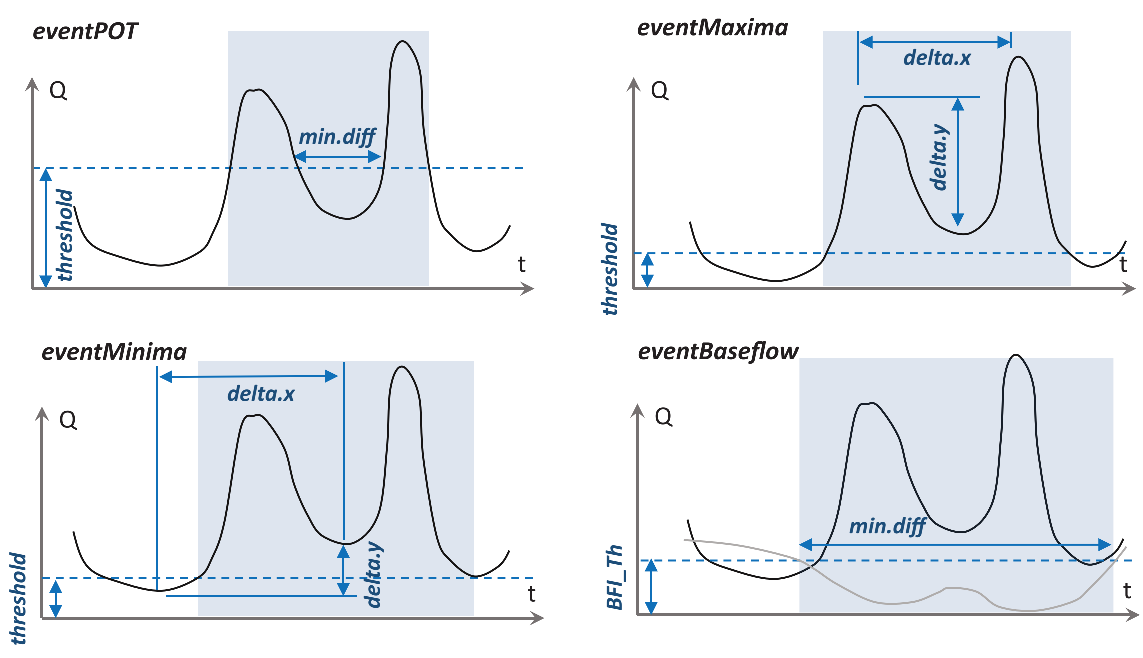

FIGURE 3 Schematic of event identification methods. The blue shading represents the identified event

neighbouring valleys calculated. If the difference between the neighbouring valleys exceeds a threshold this would characterize a new event. The methodology is similar to that in SAAS (Metcalfe and Schmidt, 2016) and AQUAPAK (Nathan et al., 2007) and is commonly used for identifying high flow events. A minimum spacing between peaks (*delta.x*) can be specified and a minimum value (*threshold*) removes leading and trailing values that may not be considered part of the event (see Figure 7-6 Linsley et al., 1958) but will not split events if a valley is below this threshold. If further splitting of events is required *eventPOT()* could be applied after *eventMaxima()*. For streamflow, independence between events for event maxima is often based on a minimum interval of 7 days (Wasko and Sharma, 2017) and a minimum difference in the maxima of successive events of 75% (Murphy et al., 2009).

3.2.3 | Local minima

Implemented in the function *eventMinima()*, neighbouring valleys are first identified and an event subsequently identified once the data has returned within an absolute difference (*delta.y*) of the first valley. This method mimics visual inspection of the data. The choice of *delta.y* will be catchment specific and the reader is referred to Tang and Carey (2017) for a detailed discussion. Similar to *eventMaxima()* an additional parameter allows filtering out small values which are not considered part of the event (*threshold*) and a minimum difference between neighbouring valleys (*delta.x*) can be specified.

3.2.4 | Proportion of baseflow contribution

Events are identified on the basis of exceeding a given baseflow index (Kaur et al., 2017), and implemented in the function *eventBaseflow()*. The baseflow index (BFI) is defined as the proportion of streamflow that occurs as baseflow. The *eventBaseflow()* function first computes the BFI for every time step of the series using *baseflowB()* (Ladson et al., 2013). Event and baseflow periods are then separated by a user-defined threshold value of BFI (*BFI_Th*). A minimum length for an event can also be specified (*min.diff*). The function defaults to a BFI threshold of 0.5.

3.3 | Event pairing

Pairing of hydrological events (for example rainfall to runoff) is performed using *pairEvents()*, in which five different specifications (*type*) of pairing are implemented within a search window (*lag*). Figure 4 summarizes the five specification types using the example of pairing rainfall to runoff:

1. From the start of the rainfall event, search forwards for a runoff peak with the window extending past the end of the rainfall plus a suitable lag.
2. From the start of the rainfall event, search forwards for the end of the runoff with the window extending past the end of the rainfall plus a suitable lag.
3. From the runoff peak, search backwards for a rainfall maximum before the start of the runoff plus a suitable lag.
4. Within a suitable window backwards from the start of the runoff search for the start of the rainfall event.
5. Within a suitable window (lag) from the rainfall peak search both forwards and backward for a runoff peak.

The function *plotPairedEvents()* is used to visualize the paired events.

4 | RESULTS AND DISCUSSION

4.1 | Baseflow separation

We present baseflow separation for 67 daily streamflow values recorded for Bass River at Loch (HRS site number 227219) in South-East Australia from 30 June 1974 to 04 September 1974. The Bass

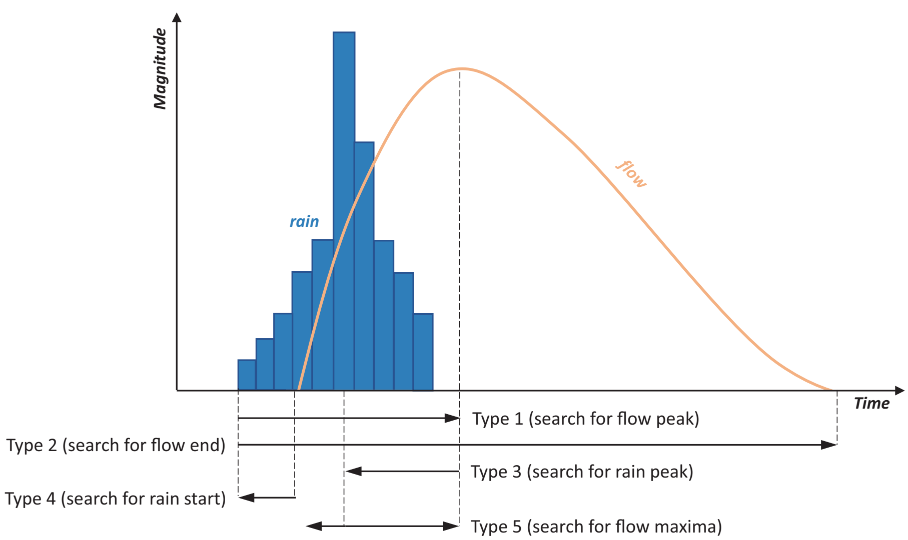

FIGURE 4 Schematic of the five event pairing algorithms implemented in function *pairEvents*. Here the example of matching rainfall (blue) to runoff (orange) is presented but the methods can be applied to any hydrologic data

River data is chosen due to its use in related literature (Grayson et al., 1996; Ladson et al., 2013) and is included in *hydroEvents* as *dataBassRiver*. As stated in Section 3.1, the majority of literature use a baseflow filter parameter (α) of 0.925 (Nathan and McMahon, 1990), though other literature suggest the use of 0.980 for the filter parameter (Ladson et al., 2013). The results of sensitivity tests to the filter parameter using three passes are presented in Figure 5.

Using *baseflowA()* with a filter parameter of 0.925 gives a baseflow index of 0.22. For the interested reader, this is the same as in *hydroStats* (Bond, 2019) and BFLOW (Arnold and Allen, 1999). Using *baseflowB()* with a filter parameter of 0.925 gives a baseflow index of 0.39 (Ladson et al., 2013) which is the same as BaseJumper (Sinclair Knight Merz, 2007) and AQUAPAK (Nathan et al., 2007). Using 0.980 in *baseflowB()* gives similar results to using 0.925 in *baseflowA()*. Previous literature (Ladson et al., 2013) suggested that differing initial values at the start and end of the flow series as well as the number of passes may be the reason for differing performance of the baseflow filters. However, our results suggest differing implementations—despite the literature suggesting both implementations are the same—are the reason behind differing baseflow indices. This means users should not simply use recommended filter parameter values from literature in combination with any baseflow filter code without verification of their choice of filter parameter. As the digital baseflow filter is not tied to any physical realism (Nathan and McMahon, 1990) and a larger fractional baseflow may aid identification of events—even if this is not strictly baseflow as per its definition (Linsley et al., 1958)—event runoff coefficient calculations for Australia (Section 4.4) use *baseflowB()* with a filter parameter of 0.925.

4.2 | Event identification

We apply the four methods (Section 3.2) for identifying events to the 67 daily streamflow values for the Bass River data presented above.

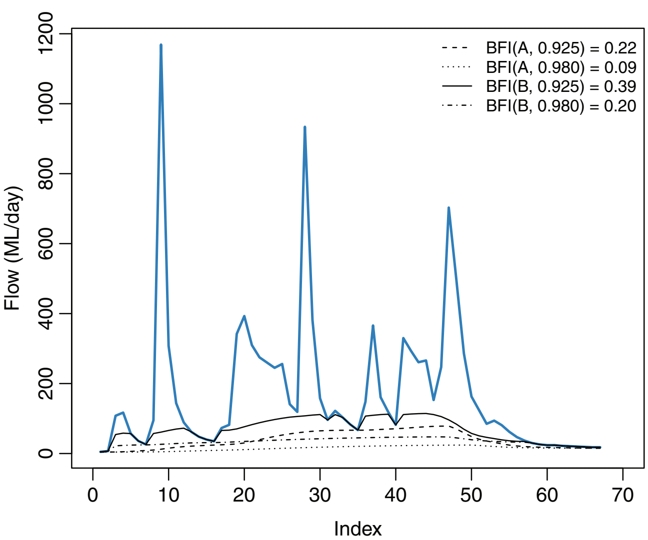

FIGURE 5 Impact of different baseflow filtering for streamflow data from 30 September 1974 to 04 September 1974 at Bass River at Loch, South-East Australia. The streamflow is shown in blue with the different baseflow filters shown in black

The results are presented in Figure 6 and are plotted using the *plotEvents()* function. Except for *eventBaseflow()* which uses a baseflow index for its separation criteria, all the event identification methods have been applied to the quickflow after removal of the baseflow using *baseflowB()*.

All the event identification methods produce plausible results but with nuanced differences. Consistent with the literature *eventPOT()* was applied using a threshold of zero meaning any streamflow above the baseflow (i.e. the quickflow) is an event. An advantage here is that small events like event (1) and (4) are identified, but a disadvantage is that events arguably that may be thought of as separate events are merged. For example, events (3) and (6) could each be split into separate events. Applying *eventMaxima()* and *eventMinima()* largely avoids the issue of unwanted merging of events. The previous single event (3) is split into events (2) and (3). Event (6) is split into three events, though using a larger vertical difference (*delta.y*) for the event identification in *eventMaxima()* would result in merging of these events once again.

Both *eventMaxima()* and *eventMinima()* fail to identify the first small peak as there is no strict minima before this event. Applying *eventBaseflow()* works well in splitting both large and small peaks in separate events and classifies the first and last small peaks as separate events. It can be generalized that, if the aim of the analysis is to identify independent streamflow maxima then *eventMaxima()* and *eventMinima()* work well and indeed have been traditionally employed for this task. If identifying independent small events becomes difficult, or the aim is to identify wet spells, *eventBaseflow()* may be preferred. The subsequent results for testing event pairing strategies uses *eventMaxima()* as it is best suited for identifying streamflow maxima. For calculating runoff coefficients across Australia events are identified using *eventBaseflow()* due to our aim of identifying a variety of event sizes.

4.3 | Event pairing

To test the different methods of pairing events from the two hydrological time-series of rainfall and runoff/streamflow we use data for HRS station 1051015A ($-15.77°$, $145.01°$) located in the tropical north of Australia (Figure 7). Rainfall events are identified using *eventPOT()* using a *threshold* $= 1$ (mm) and *min.diff* $= 1$. To present the salient differences between the pairing methods streamflow events are identified using *eventMaxima()*. Each event pair is shown in the same colour using the *plotPairs()* function.

Searching forwards in time from the start of the rainfall for a flow peak (*type* $= 1$) the first two flow peaks (shown in green) are paired to the first rainfall event. As there was no streamflow response the third rainfall event (shown in purple) remains unpaired. Where we search for the start of a streamflow event (*type* $= 2$) the last streamflow peak (shown in blue) remains unpaired. This is because the streamflow responded to rainfall which has likely not been accurately captured in the rainfall gauging of this catchment. This demonstrates the sensitivity of a pairing algorithm which only searches in the forwards direction. Pairing backwards from the streamflow peak works well (*type* $= 3$), but the algorithm cannot pair the first two streamflow

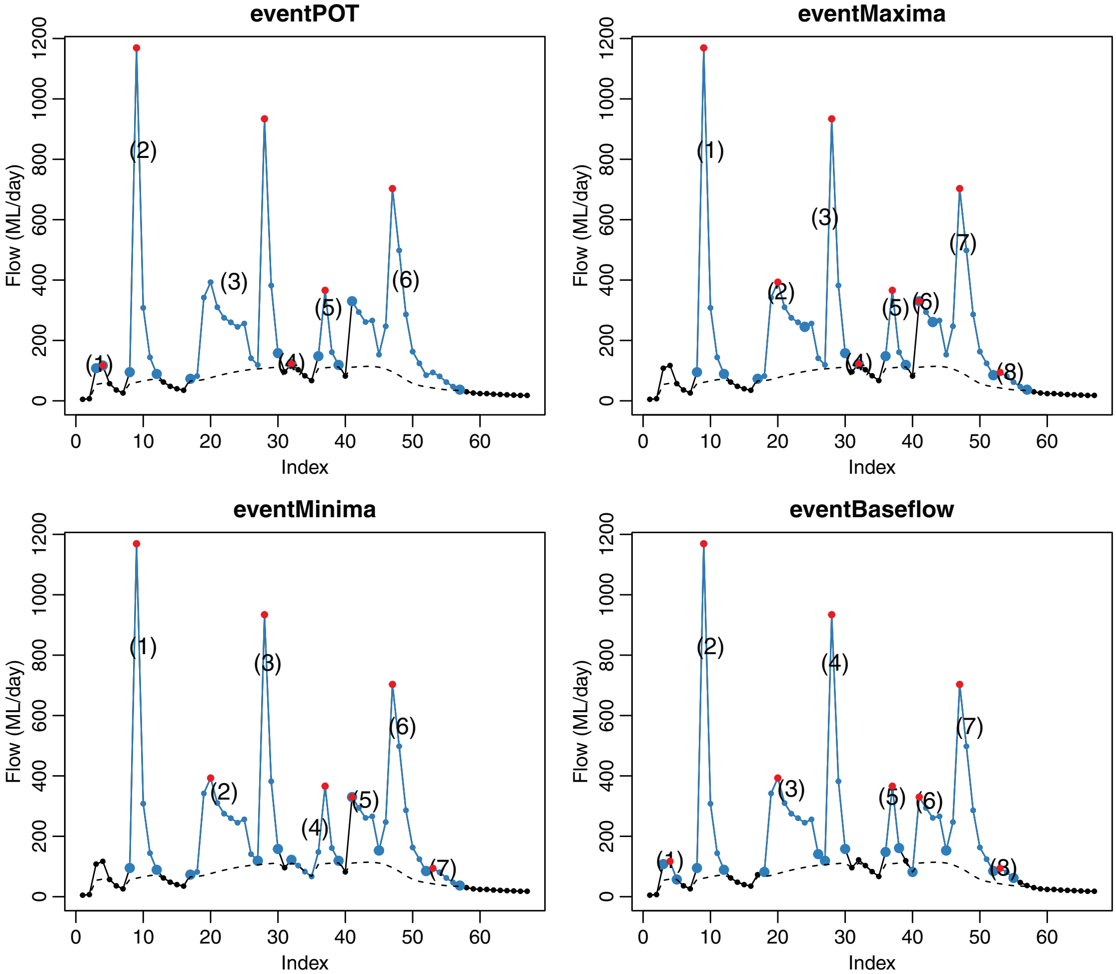

FIGURE 6 Event identification using four different methods. Events are highlighted in blue with the start and finish identified by filled circles. The numbers in brackets indicate event index. Maxima are identified using *calcStats()* and shown in red. The baseflow is indicated by a dashed line

peaks. All the rainfall (yellow) is paired only to the second streamflow peak, and not the first which remains unpaired. This is because the streamflow peaks were classified as separate events. Here the user would need to return to their event separation to ensure these two streamflow events are identified as one. As in the case of pairing forwards (*type* = 2), the final streamflow event is not paired if one searches backwards from the start of each streamflow event (*type* = 4). Interestingly the final method implemented (*type* = 5), which matches peaks in both directions, identifies event pairs well, overcoming issues which result from rainfall gauging not capturing events accurately. Not shown here, we found using *eventBaseflow()* with *BFI_Th* = 0.5 resulted in similar pairing for *type* = 1 and *type* = 2, and likewise for *type* = 3 and *type* = 4. Hence the event runoff coefficients across Australia were calculated from event pairs identified using *eventBaseflow()* with both *type* = 1 and *type* = 3 pairing algorithms.

4.4 | Event runoff coefficients for Australia

Streamflow events were identified using *eventBaseflow()* with *BFI_Th* = 0.5 and rainfall events using *eventPOT()* with *threshold* = 1 (mm) with a *min.diff* = 1 used for both streamflow and rainfall. Streamflow events were first paired to rainfall using *type* = 3 with a maximum lag equivalent to the time of concentration for individual catchments, which were estimated by the parsimonious Pilgrim McDermott formula (McDermott and Pilgrim, 1982). By passing *sum()* through *calcStats()* event runoff coefficients were calculated. Figure 8a presents the long-term average event runoff coefficients for each catchment. Event runoff coefficients greater than one were removed.

Average event runoff coefficients exhibit large variability across Australia varying from near zero to 0.7. The majority of event runoff coefficients range from near zero to 0.21 (75th percentile) indicating that when a rainfall event occurs in Australia very little of the rainfall is returned to the catchment in the form of streamflow. In the centre and south-west of Australia runoff coefficients rarely exceed 0.1. Greater event runoff coefficients are found around the north and eastern coast, correlating with regions of greater moisture availability and greater mean rainfall. The greatest event runoff coefficients are identified in the south of Australia, consistently greater than 0.2, indicating that this region of Australia has the highest proportion or rainfall returned as streamflow.

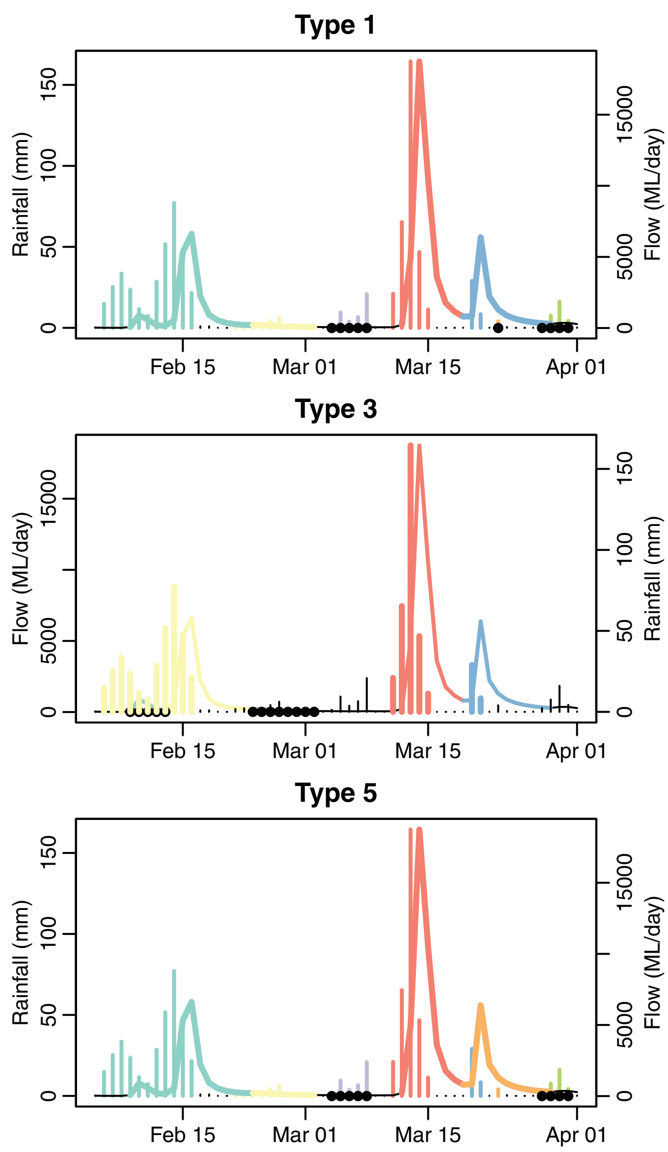

FIGURE 7 Event pairing using all five pairing specifications. The data is for the year 2015 from station 1051015A located in the tropics of Australia. Rainfall is plotted as vertical bars and the streamflow as a line. Events are coloured based on the data set being used for pairing, for example *type* = 1 pairs based on rainfall. Paired events are then indicated by the same colour and unpaired events are in black and highlighted using black circles

Event runoff coefficients are indicative of the runoff mechanism, being smallest for flash floods and increasing for short rain floods, long rain floods, rain-on-snow floods and snowmelt floods (Merz et al., 2006). This large variability in event runoff coefficients across Australia reveals interesting hydrological insights as the dominant runoff mechanisms across Australia varies little. The dominant runoff mechanisms in Australia are generally related to saturation excess overland flow rainfall whereby either rainfall falls on wet antecedent soil moisture or long (multi-day) rainfall causes the soil to wet up before overland flow occurs (Stein et al., 2020). As climatology and runoff mechanisms are the two main factors in changing event runoff coefficients (Merz et al., 2006) this suggests a large amount of the variability in event runoff coefficients may be explained by climatology (Section 4.6).

4.5 | Comparison of rainfall-runoff relationships across event and annual scales

Where event runoff coefficients are indicative of runoff mechanisms, the annual runoff ratio, aggregates catchment processes to the annual time step, and thus is a descriptor a catchment's rainfall-runoff response especially over longer temporal scales (Saft et al., 2015). Figure 8b presents the long-term mean annual runoff ratio (annual runoff divided by annual rainfall) across Australia. There is a strong similarity in the spatial pattern in the annual runoff ratio and event runoff coefficients with small values inland and in the south-west and greater values on the east coast and particularly in the south—suggesting aggregated annual rainfall-runoff relationships may be indicative of the type of runoff mechanism.

Figure 8c presents a scatter plot of the event runoff coefficient against the annual runoff ratio. The annual runoff ratios underestimate the contribution to runoff from rainfall events that exhibit runoff in catchments with very small event runoff coefficients, while overestimating the runoff contribution for the remaining catchments. For catchments with low event runoff coefficients, event runoff coefficients overestimate the streamflow response as for many rainfall events there is no streamflow response, and this behaviour is not captured by the event runoff coefficient which samples on streamflow response alone. Where the runoff response is overestimated by the annual runoff ratio there is streamflow between individual events from baseflow (groundwater) contribution that is not captured in the event response, even when baseflow is included in the event streamflow. Although annual rainfall-runoff ratios are indicative of catchment runoff response and processes they can overestimate the response from induvial events by approximately 50%.

4.6 | Sensitivity of event runoff coefficients to climate

The event runoff coefficients and annual runoff ratios are grouped by Köppen climate zone (Figure 9). Most of central Australia is arid (B) and the annual runoff ratio is very low indicating a lot of rainfall does not reach the outlet—but this underrepresents the actual catchment behaviour when there is a streamflow response. When pairing on the basis of streamflow (type = 3) the event runoff coefficients are much greater, indicating that although for many rainfall events runoff may not occur, when runoff does occur it is much greater than the annual runoff ratio may imply; this is consistent with the finding in Guo et al. (2020) for over 163 Australian catchments, in which more arid catchments are generally associated with higher skewness in runoff. This result is indicative of a strong modulation by the antecedent moisture conditions in these catchments. The same is true for the temperate dry summer (Cs) region whereby catchments spend much time being wetted up in the wet season before runoff and high flows occur (Wasko et al., 2020b).

In the temperate dry winter (Cw) and tropical (A) regions, the reverse is true with event runoff coefficients much less than annual runoff ratios. For these climates, although antecedent moisture conditions modulate runoff response there are equal contributions from rainfall and antecedent soil moisture to the runoff response (Wasko et al., 2020b) suggesting a contribution from infiltration excess as a runoff mechanism. As many rivers remain ephemeral, there is a streamflow (baseflow) contribution between rainfall events that is not included in the event runoff coefficient, resulting in the greater annual

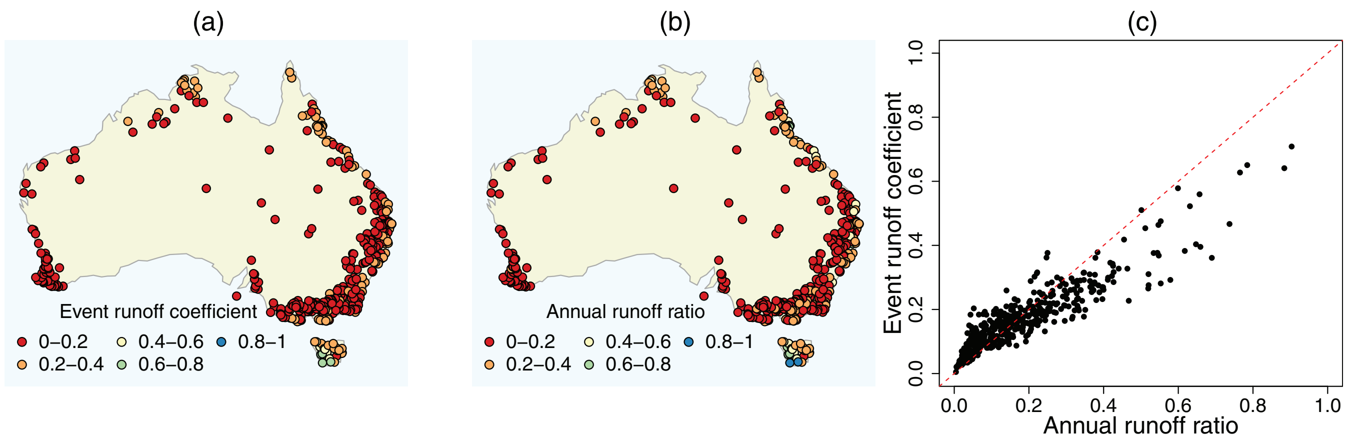

FIGURE 8 Comparison of event runoff coefficients and annual runoff ratio for Australia (a) event runoff coefficient (b) annual rainfall ratio (c) scatterplot of event runoff coefficient and annual runoff ratios

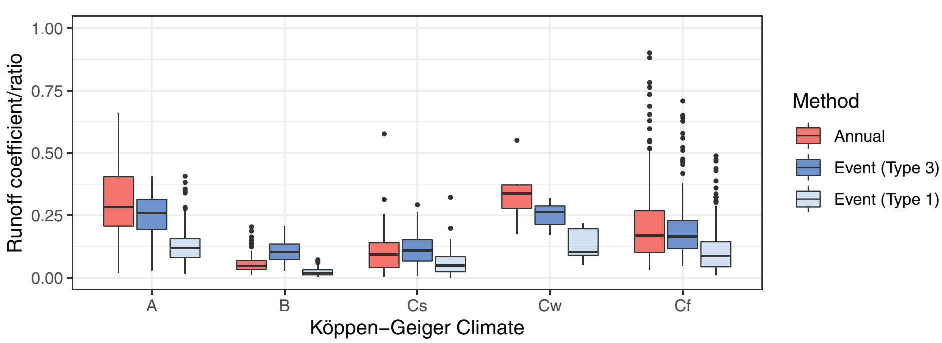

FIGURE 9 Event runoff coefficients and annual rainfall-runoff relationships for Australia by climate zone. A—Tropical; B—Arid; Cs—Temperate dry summer; Cw—Temperate dry winter; Cf—Temperate no dry season

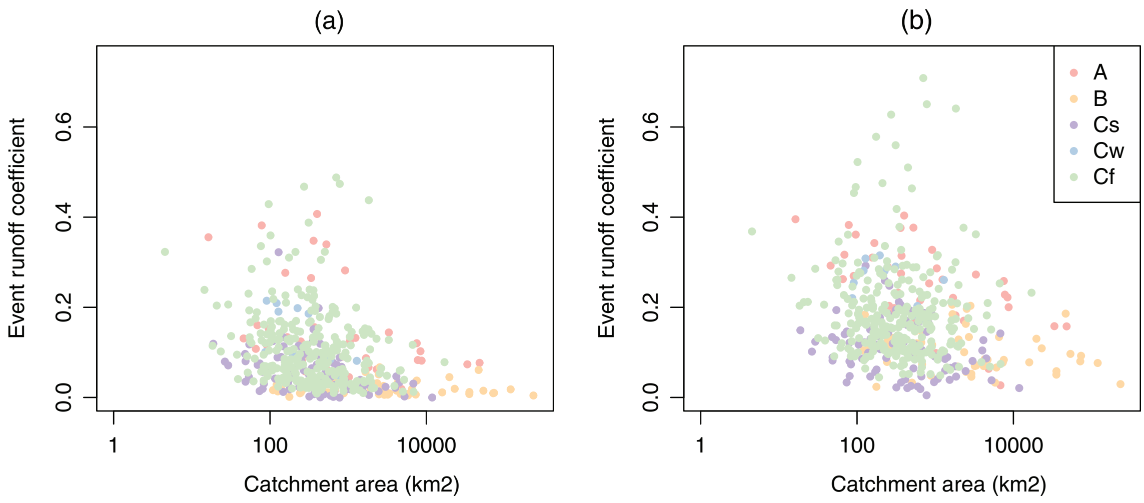

FIGURE 10 Event runoff coefficients versus catchment area (a) sampling based on rainfall (type = 1) (b) sampling based on runoff (type = 3). The circle colour indicates the climate zone. A—Tropical; B—Arid; Cs—Temperate dry summer; Cw—Temperate dry winter; Cf—Temperate no dry season

runoff ratio. It does not appear that this baseflow contributes significantly to the flood response as otherwise the event runoff coefficient and annual runoff ratio would be more similar.

In the temperate no dry season (Cf) climate zone, we see similar event runoff coefficients and annual runoff coefficients due to perennial rivers and the annual runoff contribution being strongly related to the event-based runoff. We note though that floods in the temperate no dry season climate zone (south-east of Australia) are winter dominant, despite rainfall extremes occurring throughout the year, due to rainfall excess flooding resulting from wet antecedent soil (Wasko et al., 2020b). Hence the seasonality of the different climate zones plays a large role in the runoff mechanism affecting Australia. In addition, if one was to rank the climate zones in terms of their runoff response, based on annual runoff ratios one might rank arid and temperate dry summer as having different behaviour, but in fact, our results showed that their runoff behaviour is very similar based on the event runoff coefficient, with a strong rainfall excess flow mechanism.

4.7 | Sensitivity of event runoff coefficients to catchment area and pairing strategy

Different sampling and pairing strategies, as well as catchment properties, will lead to the calculation of different event runoff coefficients and hence possible misidentification of runoff generation processes. Although the relative ranking of event runoff coefficients across climates remains consistent (Figure 9), when pairing on the basis of rainfall (*type* = 1) the event runoff coefficients are consistently less than when paired on the basis of streamflow (*type* = 3). This is because events with wet antecedence and greater event magnitude are more likely to be chosen when pairing on the basis on the streamflow. Sampling on the basis of streamflow induces a bias to sampling events with saturated excess streamflow and results in a much greater streamflow response being implied from a rainfall event than one could actually expect. This sensitivity to pairing strategy and climatology is further stratified on catchment area (Figure 10). The event runoff coefficient decreases as catchment area increases (Cerdan et al., 2004), with the larger the catchment, the less variability in the event runoff coefficient. This behaviour is consistent across different climate zones and sampling strategies.

The variability induced by the choice of pairing strategy is no less than the variability across climate zones and greater than the differences between annual and event approaches. When paired on the basis of rainfall, the event runoff coefficients exhibit much less variability demonstrating how in fact many of the climate zones behave similarly in terms of runoff mechanism with strong modulation of flood response due to dry antecedent moisture conditions and the moisture limited nature of the Australia continent (Anabalón and Sharma, 2017). Although the dominant runoff generation processes remain well represented by both pairing strategies, these results highlight that the approach used to pair events can have more of an impact on the magnitude of event runoff coefficients than the primary driver of runoff variability in Australia, that is, the climatology.

5 | CONCLUSIONS

Here we used the *R* package *hydroEvents* to identify and pair rainfall and streamflow events to compile the first ever evaluation of event-scale rainfall-runoff relationships across the continent of Australia. As the *hydroEvents* package implements four different methods of identifying events and five different methods of pairing events, each was first tested before subsequent calculation of event runoff coefficients. For calculating the baseflow contribution, sensitivity testing indicated that, despite similar descriptions, the baseflow filters did not work identically. It is hence suggested that one should not simply use a recommended filter parameter values from literature in combination with any baseflow filter implementation without verification of the resulting baseflow index.

The *hydroEvents* package implements four methods of identifying events based on (1) peaks over threshold, (2) event maxima, (3) event minima and (4) a baseflow index. It was found that, although each method can give similar results depending on the parametrisation, for identification of streamflow maxima a method based on local maxima or minima is preferred, but where small events or wet spells are a target, a method using the baseflow index may be preferable.

Five approaches to pairing events between two time-series (e.g. rainfall and runoff) incorporating different search directions and start/end points were tested. Pairing forwards on the basis of rainfall may miss events where the streamflow responded to rainfall which has not been accurately captured in the rainfall gauging of the catchment. Alternatively, pairing backwards from streamflow can fail to match multiple rainfall peaks requiring careful sampling of rainfall events. Matching peaks in both directions can overcome issues which result from rainfall gauging not capturing events accurately.

We presented the first continental analysis of event-scale rainfall-runoff relationships for Australia. Using the proportion of baseflow contribution (baseflow index) to identify runoff events, and a peak over a threshold to identifying precipitation events, event runoff coefficients across Australia were calculated. Two pairing strategies were tested—pairing forwards from the rainfall and pairing backwards from the resultant runoff. Event runoff coefficients for Australia indicate that little rainfall is returned to runoff across the Australian continent with climatic variability being the primary driver of event runoff response. With the exception of the tropics most runoff is generated due to rainfall excess whereby runoff is generated by rainfall falling on wet ground. The impact of analysis choice was presented by calculating event runoff coefficients pairing rainfall runoff events on the basis of runoff, and then on the basis of rainfall, with markedly differing results. Sampling on the basis of streamflow induces a bias to sampling events wet antecedent moisture and results in a much greater streamflow response being implied from a rainfall event than one would expect is predicting the runoff response based on rainfall sampling.

The *hydroEvents* package is the only open-source package to apply multiple event identification and pairing methodologies. We note that although we illustrated the use of *hydroEvents* package on rainfall and runoff time-series, the package is flexible enough to identify and pair events in many hydrological variables, such as compound extremes resulting from rainfall and positive tidal anomaly. The *hydroEvents* package will enable efficient analysis of large data sets, facilitate replicability of future studies, and lead to improved understanding of hydrological processes.

ACKNOWLEDGEMENTS

Conrad Wasko receives funding from Australian Research Council (DE210100479). Open access publishing facilitated by The University of Melbourne, as part of the Wiley - The University of Melbourne agreement via the Council of Australian University Librarians. [Correction added on 18 May 2022, after first online publication: CAUL funding statement has been added.]

DATA AVAILABILITY STATEMENT

The Bass River data were published in Grayson et al. (1996). Streamflow data are from the Australian Bureau of Meteorology Hydrological Reference Station (HRS) dataset, available from http://www.bom.gov.au/water/hrs/ and are described in Zhang et al. (2016). Catchment average daily rainfall is from Australian Water Availability Project (Jones et al., 2009) and extracted using the R package AWAPer (Peterson et al., 2020). Analysis was performed using the R package hydroEvents (Wasko and Guo, 2021) available via CRAN at https://CRAN.R-project.org/package=hydroEvents

ORCID

Conrad Wasko https://orcid.org/0000-0002-9166-8289
Danlu Guo https://orcid.org/0000-0003-1083-1214

REFERENCES

Anabalón, A., & Sharma, A. (2017). On the divergence of potential and actual evapotranspiration trends: An assessment across alternate global datasets. *Earth's Future*, *5*(9), 905–917. https://doi.org/10.1002/2016EF000499

Andrews, F. T., Croke, B. F. W., & Jakeman, A. J. (2011). An open software environment for hydrological model assessment and development. *Environmental Modelling & Software*, *26*(10), 1171–1185. https://doi.org/10.1016/j.envsoft.2011.04.006

Arnold, J. G., & Allen, P. M. (1999). Automated methods for estimating baseflow and ground water recharge from streamflow records. *Journal of the American Water Resources Association*, *35*(2), 411–424. https://doi.org/10.1111/j.1752-1688.1999.tb03599.x

Beck, H. E., Van Dijk, A. I. J. M., Miralles, D. G., De Jeu, R. A. M., Bruijnzeel, L. A., McVicar, T. R., & Schellekens, J. (2013). Global patterns in base flow index and recession based on streamflow observations from 3394 catchments. *Water Resources Research*, *49*(12), 7843–7863. https://doi.org/10.1002/2013WR013918

Beck, H. E., Zimmermann, N. E., McVicar, T. R., Vergopolan, N., Berg, A., & Wood, E. F. (2018). Present and future köppen-Geiger climate classification maps at 1-km resolution. *Scientific Data*, *5*, 180214. https://doi.org/10.1038/sdata.2018.214

Bende-Michl, U., Verburg, K., & Cresswell, H. P. (2013). High-frequency nutrient monitoring to infer seasonal patterns in catchment source availability, mobilisation and delivery. *Environmental Monitoring and Assessment*, *185*(11), 9191–9219. https://doi.org/10.1007/s10661-013-3246-8

Blume, T., Zehe, E., & Bronstert, A. (2007). Rainfall-runoff response, event-based runoff coefficients and hydrograph separation. *Hydrological Sciences Journal*, *52*(5), 843–862. https://doi.org/10.1623/hysj.52.5.843

Bond N. 2019. hydrostats: Hydrologic Indices for Daily Time Series Data, R package version 0.2.7. [available at https://cran.r-project.org/web/packages/hydrostats/index.html].

Boughton, W. (1993). A hydrograph-based model for estimating the water yield of ungauged catchments. In *Hydrology and water resources symposium* (pp. 317–324). Engineers Australia.

Brodtkorb, P. A., Johannesson, P., Lindgren, G., Rychlik, I., Rydén, J., & Sjö, E. (2000). WAFO - a Matlab toolbox for analysis of random waves and loads. In *The tenth international offshore and polar engineering ConferenceSeattle*. OnePetro. (pp. 343–350).

Cerdan, O., Le Bissonnais, Y., Govers, G., Lecomte, V., Van Oost, K., Couturier, A., King, C., & Dubreuil, N. (2004). Scale effect on runoff from experimental plots to catchments in agricultural areas in Normandy. *Journal of Hydrology*, *299*(1–2), 4–14. https://doi.org/10.1016/j.jhydrol.2004.02.017

Chen, H., & Teegavarapu, R. (2019). Comparative analysis of four Baseflow separation methods in the South Atlantic-gulf region of the U.S. *Water*, *12*(1), 120. https://doi.org/10.3390/w12010120

Dierauer, J., & Whitfield, P. (2019). FlowScreen: Daily Streamflow Trend and Change Point Screening. IET. *R package version 1.2.6*. [available at. https://cran.r-project.org/web/packages/FlowScreen/index.html

Dunkerley, D. (2008). Identifying individual rain events from pluviograph records: A review with analysis of data from an Australian dryland site. *Hydrological Processes*, *22*(26), 5024–5036. https://doi.org/10.1002/hyp.7122

Duque, L. F. (2020). IETD: Inter-Event Time Definition. *R package version 1.0.0*. [available at. https://cran.r-project.org/web/packages/IETD/index.html

Eckhardt, K. (2005). How to construct recursive digital filters for baseflow separation. *Hydrological Processes*, *19*(2), 507–515. https://doi.org/10.1002/hyp.5675

Eckhardt, K. (2008). A comparison of baseflow indices, which were calculated with seven different baseflow separation methods. *Journal of Hydrology*, *352*(1–2), 168–173. https://doi.org/10.1016/j.jhydrol.2008.01.005

Eckhardt, K. (2012). Technical note: Analytical sensitivity analysis of a two parameter recursive digital baseflow separation filter. *Hydrology and Earth System Sciences*, *16*(2), 451–455. https://doi.org/10.5194/hess-16-451-2012

Frazier, P., Page, K., Louis, J., Briggs, S., & Robertson, A. I. (2003). Relating wetland inundation to river flow using Landsat TM data. *International Journal of Remote Sensing*, *24*(19), 3755–3770. https://doi.org/10.1080/0143116021000023916

Fuka, D. R., Walter, M. T., Archibald, J. A., Stenhuis, T. S., & Easton, Z. M. (2018). EcoHydRology: A Community Modeling Foundation for Eco-Hydrology. *R package version 0.4.12.1*. [available at. https://cran.r-project.org/web/packages/EcoHydRology/index.html

Grayson, R., Argent, R. M., Nathan, R. J., McMahon, T. A., & Mein, R. G. (1996). *Hydrological Recipes*. Cooperative Reserach Centre for Catchment Hydrology.

Guo, D., Minaudo, C., Lintern, A., Bende-Michl, U., Liu, S., Zhang, K., & Duvert, C. (2022). Synthesizing the impacts of baseflow contribution on concentration-discharge (C-Q) relationships across Australia using a Bayesian hierarchical model. *Hydrology and Earth System Sciences*, *26*(1), 1–16. https://doi.org/10.5194/hess-26-1-2022

Guo, D., Zheng, F., Gupta, H., & Maier, H. R. (2020). On the robustness of conceptual rainfall-runoff models to calibration and evaluation data set splits selection: A large sample investigation. *Water Resources Research*, *56*(3), e2019WR026752. https://doi.org/10.1029/2019WR026752

Hewlett, J. D., & Hibbert, A. R. (1967). Factors affecting the response of small watersheds to precipitation in humid areas. *Forest Hydrology*, *33*(2), 288–293. https://doi.org/10.1177/0309133309338118

Hettiarachchi, S., Wasko, C., & Sharma, A. (2022). Do longer dry spells associated with warmer years compound the stress on global water resources? *Earth's Futur*, *10*, e2021EF002392. https://doi.org/10.1029/2021EF002392

Jones D, Wang W, & Fawcett R. (2009). High-quality spatial climate data-sets for Australia. *Aust. Meteorol. Oceanogr. J.*, *58*, 233–248. Available at: http://scholar.google.com/scholar?hl=en&btnG=Search&q=intitle:High-quality+spatial+climate+data-sets+for+Australia#0 [Accessed 31 October 2012]

Joo, J., Lee, J., Kim, J. H., Jun, H., & Jo, D. (2014). Inter-event time definition setting procedure for urban drainage systems. *Water*, *6*(1), 45–58. https://doi.org/10.3390/w6010045

Kaur, S., Horne, A., Stewardson, M. J., Nathan, R., Costa, A. M., Szemis, J. M., & Webb, J. A. (2017). Challenges for determining frequency of high flow spells for varying thresholds in environmental flows programmes. *Journal of Ecohydraulics*, *2*(1), 28–37. https://doi.org/10.1080/24705357.2016.1276418

Kirchner, J. W. (2009). Catchments as simple dynamical systems: Catchment characterization, rainfall-runoff modeling, and doing hydrology backward. *Water Resources Research*, *45*(2), W02429. https://doi.org/10.1029/2008WR006912

Koffler D, Gauster T, Laaha G. 2016. lfstat: Calculation of Low Flow Statistics for Daily Stream Flow Data, R package version 0.9.4. [available at https://cran.r-project.org/web/packages/lfstat/index.html].

Ladson, A., Brown, R., Neal, B., & Nathan, R. (2013). A standard approach to baseflow separation using the Lyne and Hollick filter. *Australian Journal of Water Resources*, *17*(1), 25–34. https://doi.org/10.7158/W12-028.2013.17.1

Leonard, M., Westra, S., Phatak, A., Lambert, M., van den Hurk, B., Mcinnes, K., Risbey, J., Schuster, S., Jakob, D., & Stafford-Smith, M. (2014). A compound event framework for understanding extreme impacts. *Wiley Interdisciplinary Reviews: Climate Change*, *5*(1), 113–128. https://doi.org/10.1002/wcc.252

Li, L., Maier, H. R., Lambert, M. F., Simmons, C. T., & Partington, D. (2013). Framework for assessing and improving the performance of recursive digital filters for baseflow estimation with application to the Lyne and Hollick filter. *Environmental Modelling & Software*, *41*, 163–175. https://doi.org/10.1016/j.envsoft.2012.11.009

Linsley, R. K., Kohler, M. A., & Paulhus, J. L. (1958). *Hydrology for engineers*. McGraw-Hill. https://doi.org/10.1016/0022-1694(84)90195-1

Lyne V, Hollick M. (1979). *Stochastic time-variable rainfall-runoff modelling*. In: Institute of Engineers Australia National Conference. Barton, Australia: Institute of Engineers Australia, pp. 89–92. Available at: file:///R:/LITERATURE/Jasmine/Lyne&Hollick (1979) - baseflow separation, rainfall-runoff.pdf

McDermott, G. E., & Pilgrim, D. H. (1982). *Design flood estimation for small catchments in*. New South Wales. Australian Water Resources Council Technical Paper No. 73. Australian Government Publishing Service.

McMahon, T. A., & Nathan, R. J. (2021). Baseflow and transmission loss: A review. *Wiley Interdisciplinary Reviews: Water*, *8*(4), e1527. https://doi.org/10.1002/wat2.1527

Merz, B., Vorogushyn, S., Uhlemann, S., Delgado, J., & Hundecha, Y. (2012). HESS opinions: 'More efforts and scientific rigour are needed to attribute trends in flood time series'. *Hydrology and Earth System Sciences*, *16*(5), 1379–1387. https://doi.org/10.5194/hess-16-1379-2012

Merz, R., Blöschl, G., & Parajka, J. (2006). Spatio-temporal variability of event runoff coefficients. *Journal of Hydrology*, *331*(3–4), 591–604. https://doi.org/10.1016/j.jhydrol.2006.06.008

Metcalfe RA, Schmidt BJ. 2016. Streamflow Analysis and Assessment Software (version 4.1)

Minaudo, C., Dupas, R., Gascuel-Odoux, C., Roubeix, V., Danis, P. A., & Moatar, F. (2019). Seasonal and event-based concentration-discharge relationships to identify catchment controls on nutrient export regimes. *Advances in Water Resources*, *131*, 103379. https://doi.org/10.1016/j.advwatres.2019.103379

Nathan, R. J., & McMahon, T. A. (1990). Evaluation of automated techniques for base flow and recession analyses. *Water Resources Research*, *26*(7), 1465–1473. https://doi.org/10.1029/WR026i007p01465

Nathan RJ, Gordon N, McMahon TA, Finlayson BL, Gippel CJ. 2007. *AQUAPAK (version 1.05)*. [available at https://www.jacobs.com/natural-resource-management].

O'Shea, D., Nathan, R., Wasko, C., & Hill, P. (2021). Implications of event-based loss model structure on simulating large floods. *Journal of Hydrology*, *595*(May 2020), 126008. https://doi.org/10.1016/j.jhydrol.2021.126008

Partington D, Brunner P, Simmons CT, Werner AD, Therrien R, Maier HR, Dandy GC. (2012). Evaluation of outputs from automated baseflow separation methods against simulated baseflow from a physically based, surface water-groundwater flow model. *Journal of Hydrology*, *458–459*. 28–39 DOI: https://doi.org/10.1016/j.jhydrol.2012.06.029

Pelletier, A., & Andréassian, V. (2020). Hydrograph separation: An impartial parametrisation for an imperfect method. *Hydrology and Earth System Sciences*, *24*(3), 1171–1187. https://doi.org/10.5194/hess-24-1171-2020

Pelletier A, Andreassian V, Delaigue O. (2021). baseflow: Computes Hydrograph Separation, R package version 0.13.2. [available at https://cran.r-project.org/web/packages/baseflow/index.html]. DOI: 10.15454/Z9IK5N

Peterson, T. J., Saft, M., Peel, M. C., & John, A. (2021). Watersheds may not recover from drought. *Science*, *372*(6543), 745–749. https://doi.org/10.1126/science.abd5085

Peterson, T. J., Wasko, C., Saft, M., & Peel, M. C. (2020). AWAPer: An R package for area weighted catchment daily meteorological data anywhere within Australia. *Hydrological Processes*, *34*(5), 1301–1306. https://doi.org/10.1002/hyp.13637

Raudkivi, A. J. (1979). INTRODUCTION. In *Hydrology: An advanced Introduction to hydrological processes and Modelling*. Pergamon.

Razavi, S., Gober, P., Maier, H. R., Brouwer, R., & Wheater, H. (2020). Anthropocene flooding: Challenges for science and society. *Hydrological Processes*, *34*(8), 1996–2000. https://doi.org/10.1002/hyp.13723

Saft, M., Peel, M. C., Western, A. W., & Zhang, L. (2016). Predicting shifts in rainfall-runoff partitioning during multiyear drought: Roles of dry period and catchment characteristics. *Water Resources Research*, *52*(12), 9290–9305. https://doi.org/10.1002/2016WR019525

Saft, M., Western, A. W., Zhang, L., Peel, M. C., & Potter, N. J. (2015). The influence of multiyear drought on the annual rainfall-runoff relationship: An Australian perspective. *Water Resources Research*, *51*(4), 2444–2463. https://doi.org/10.1002/2014WR015348

Sikorska, A. E., Viviroli, D., & Seibert, J. (2015). Flood-type classification in mountainous catchments using crisp and fuzzy decision trees. *Water Resources Research*, *51*(10), 7959–7976. https://doi.org/10.1002/2015WR017326

Sinclair Knight Merz. 2007. Using baseflow for monitoring stream condition and groundwater and surface water resource condition change

Stein, L., Pianosi, F., & Woods, R. (2020). Event-based classification for global study of river flood generating processes. *Hydrological Processes*, *34*(7), 1514–1529. https://doi.org/10.1002/hyp.13678

Stoelzle, M., Stahl, K., & Weiler, M. (2013). Are streamflow recession characteristics really characteristic? *Hydrology and Earth System Sciences*, *17*(2), 817–828. https://doi.org/10.5194/hess-17-817-2013

von Storch, H. (1999). Misuses of statistical analysis in climate research. In *Analysis of Climate Variability* (pp. 11–26). Springer. https://doi.org/10.1007/978-3-662-03744-7_2

Tallaksen, L. M., & van Lanen, H. A. J. (2004). *Hydrological drought: Processes and estimation methods for streamflow and groundwater*. Elsevier.

Tang, W., & Carey, S. K. (2017). HydRun: A MATLAB toolbox for rainfall–runoff analysis. *Hydrological Processes*, *31*(15), 2670–2682. https://doi.org/10.1002/hyp.11185

Tarasova, L., Basso, S., Zink, M., & Merz, R. (2018). Exploring controls on rainfall-runoff events: 1. Time series-based event separation and temporal dynamics of event runoff response in Germany. *Water Resources Research*, *54*(10), 7711–7732. https://doi.org/10.1029/2018WR022587

Tonkin, J. D., Poff, N. L., Bond, N. R., Horne, A., Merritt, D. M., Reynolds, L. V., Olden, J. D., Ruhi, A., & Lytle, D. A. (2019). Prepare river ecosystems for an uncertain future. *Nature*, *570*(7761), 301–303. https://doi.org/10.1038/d41586-019-01877-1

Tramblay, Y., Bouvier, C., Martin, C., Didon-Lescot, J. F., Todorovik, D., & Domergue, J. M. (2010). Assessment of initial soil moisture conditions for event-based rainfall-runoff modelling. *Journal of Hydrology*, *387*(3–4), 176–187. https://doi.org/10.1016/j.jhydrol.2010.04.006

Vogel, E., Donat, M. G., Alexander, L. V., Meinshausen, M., Ray, D. K., Karoly, D., Meinshausen, N., & Frieler, K. (2019). The effects of climate extremes on global agricultural yields. *Environmental Research Letters*, *14*, 054010. https://doi.org/10.1088/1748-9326/ab154b

Wasko C, Guo D. 2021. hydroEvents: Extract Event Statstics in Hydrologic Time Series, R package version 0.10. [available at https://CRAN.R-project.org/package=hydroEvents].

Wasko, C., & Nathan, R. (2019). Influence of changes in rainfall and soil moisture on trends in flooding. *Journal of Hydrology*, *575*(November 2018), 432–441. https://doi.org/10.1016/j.jhydrol.2019.05.054

Wasko, C., Nathan, R., & Peel, M. C. (2020a). Trends in global flood and Streamflow timing based on local water year. *Water Resources Research*, *56*(8), e2020WR027233. https://doi.org/10.1029/2020WR027233

Wasko, C., Nathan, R., & Peel, M. C. (2020b). Changes in antecedent soil moisture modulate flood seasonality in a changing climate. *Water Resources Research*, *56*(3), e2019WR026300. https://doi.org/10.1029/2019WR026300

Wasko, C., Sharma, A., & Pui, A. (2021a). Linking temperature to catastrophe damages from hydrologic and meteorological extremes. *Journal of Hydrology*, *602*, 126731. https://doi.org/10.1016/j.jhydrol.2021.126731

Wasko, C., Westra, S., Nathan, R., Orr, H. G., Villarini, G., Villalobos Herrera, R., & Fowler, H. J. (2021b). Incorporating climate change in flood estimation guidance. *Philosophical Transactions of the Royal Society A: Mathematical, Physical and Engineering Sciences*, *379*(2195), 20190548. https://doi.org/10.1098/rsta.2019.0548

Wasko, C., Visser, J. B., Nathan, R., Ho, M., Sharma, A. (2022). Automating rainfall recording: ensuring homogeneity when instruments change. *J. Hydrol*, *609*, 127758. https://doi.org/10.1016/j.jhydrol.2022.127758

Yao, L., Sankarasubramanian, A., & Wang, D. (2021). Climatic and landscape controls on long-term Baseflow. *Water Resources Research*, *57*(6), e2020WR029284. https://doi.org/10.1029/2020wr029284

Zhang, J., Zhang, Y., Song, J., Cheng, L., Kumar Paul, P., Gan, R., Shi, X., Luo, Z., & Zhao, P. (2020). Large-scale baseflow index prediction using hydrological modelling, linear and multilevel regression approaches. *Journal of Hydrology*, *585*, 124780. https://doi.org/10.1016/j.jhydrol.2020.124780

Zhang, X. S., Amirthanathan, G. E., Bari, M. A., Laugesen, R. M., Shin, D., Kent, D. M., MacDonald, A. M., Turner, M. E., & Tuteja, N. K. (2016). How streamflow has changed across Australia since the 1950s: Evidence from the network of hydrologic reference stations. *Hydrology and Earth System Sciences*, *20*(9), 3947–3965. https://doi.org/10.5194/hess-20-3947-2016

Zimmer, M. A., & McGlynn, B. L. (2017). Bidirectional stream–groundwater flow in response to ephemeral and intermittent streamflow and groundwater seasonality. *Hydrological Processes*, *31*(22), 3871–3880. https://doi.org/10.1002/hyp.11301

How to cite this article: Wasko, C., & Guo, D. (2022). Understanding event runoff coefficient variability across Australia using the *hydroEvents R* package. *Hydrological Processes*, *36*(4), e14563. https://doi.org/10.1002/hyp.14563